THE JOURNAL OF PHYSICAL CHEMISTRY C

pubs.acs.org/JPCC

Article

Chemical Interface Damping as an Indicator for Hexadecyltrimethylammonium Bromide Replacement by Short-Chain Thiols on Gold Nanorods

Dániel P. Szekrényes, Dávid Kovács, Zsolt Zolnai, and András Deák*

Cite This: J. Phys. Chem. C 2020, 124, 19736–19742

Read Online

ACCESS | Metrics & More | Article Recommendations | Supporting Information

ABSTRACT: The binding of thiols on hexadecyltrimethylammonium bromide (CTAB)-capped gold nanorods is investigated both at the ensemble and individual particle level using two similar sized but oppositely charged small molecules, namely, cysteamine and mercaptopropionic acid (MPA). Changes in the width and position of the localized surface plasmon resonance of individual gold nanorods are used to elucidate differences between the accumulation of these two short-chain thiols at the particles' surface. It is shown that the interplay between the charged nature of the thiol molecules and the concentration of CTAB in the bulk phase determines to which extent the thiols bind to the particles. On the basis of the changes in the resonance widths, the binding of the negatively charged MPA is reduced compared to that of the positively charged cysteamine, especially at higher CTAB bulk concentrations. This is interpreted as the result of the interaction between the small molecule thiols and CTAB: while cysteamine is effectively replacing CTAB, the interaction of readily bound MPA and CTAB from the bulk results in a self-limiting process.

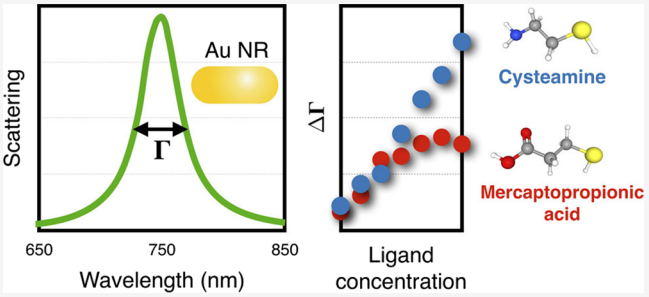

INTRODUCTION

Wet-chemical surface modification of nanoparticles is of central importance not only for practical applications, but also for fundamental studies. A proper surface layer is one of the key factors determining how and to what purpose liquid-dispersed nanoscale particles might be used. Chemically synthesized nanoparticles intrinsically feature surface attached ligands which are indispensable for the yield, quality and colloidal stability of particles. To enable their efficient use, the surface ligand layer has to be modified or replaced. The strong gold-sulfur bond provides a convenient way for a myriad of surface modification strategies[1] that have been exploited with great success over the past few decades and led to widespread interest in gold nanoparticles with various sizes and shapes as well as in their assemblies. This interest is also because these gold nanoparticles can support localized surface plasmon resonance (LSPR), allowing a range of innovative application from sensing to energy harvesting.[2,3] These resonance modes result in a fairly sharp peak in the extinction spectrum of the particles. The wavelength position and the width of this peak is affected primarily by the size and shape of the particles as well as the dielectric function of their environment.[4] Experimental optical studies performed on individual nanoparticles are of fundamental importance, as they are not affected by inhomogeneous line broadening and hence allow more rigorous comparison with theoretical models and simulation data.[5] For instance, as the localized plasmon resonance can be approximated as a dipole antenna, the scattering spectra of individual particles can be conveniently analyzed based on the damped harmonic oscillator model that—in spite of its simplicity—can provide a deeper insight into the factors that affect the resonance. A Lorentz-function fitted to the individual particles' scattering spectrum provides the resonance energy and damping of the model dipole-oscillator. These parameters are determined by factors that have an impact on the frequency or decay mechanism of the localized plasmon oscillation.[6] Recently, a new aspect of the thiol molecule-related gold nanoparticle surface modification came into focus by analyzing the scattering spectrum of individual gold nanorods. Experimental findings indicate that the width of the resonance (or damping, in terms of the oscillator model) systematically increases as thiols bind to the surface and is referring to as chemical interface damping (CID) in terms of an energy loss channel of the damped oscillator.[6] While there are different concepts regarding the underlying physical process—including electron scattering on mirror dipoles under the particle surface[7] and direct electron transfer between the particle and

Received: May 22, 2020
Revised: July 14, 2020
Published: August 17, 2020

https://dx.doi.org/10.1021/acs.jpcc.0c04629
J. Phys. Chem. C 2020, 124, 19736–19742

the thiol[8]—its contribution to the surface damping of the nanorods results in the broadening of the resonance peak. Additionally, it is argued that it also correlates with the chemical enhancement in the surface-enhanced Raman scattering process.[9,10] The increasing CID-associated peak broadening has been readily employed to indicate thiol molecule accumulation on gold nanoparticles, with the priority to clarify the origin and mechanism of the CID process.[7,8,11−13] Consequently, these studies deal with nanoparticles where the original capping layer (typically CTAB) has been previously removed and the thiols are adsorbed at the cleaned particle interface. In terms of treating the localized plasmons as a damped harmonic oscillator, the width of the resonance peak (damping) is determined by contributions from the different energy loss channels. Besides the bulk, interband, and radiation damping, the surface contribution (Γ_s) has to be taken into account, which is usually given by the expression Av_F/L_{eff}, where v_F is the Fermi velocity of the conduction band electrons, L_{eff} is the effective path length of electrons to the surface, and A is an effective proportionality factor to be experimentally determined. In arbitrary shaped particles L_{eff} is calculated as $L_{eff} = 4\ V/S$, where V and S stand for the volume and surface of the nanoparticle, respectively.[6] This energy loss channel is related to the scattering of the oscillating electrons at the interface. Along the same concept, this term also includes the chemical interface contribution, Γ_{CID}, which is due to chemically bound molecules and has a proportionality factor A_{CID}. The value of A_{CID} might depend on the type of molecules that bind to the gold particles,[11] and additionally changes in Γ_{CID} (hence in the effective A_{CID} as well) will depend on the actual coverage of the particles, as shown by several recent experimental studies.[11,12,14,15]

In this work our aim is to elucidate how the concept of damping increase because of thiol binding in combination with the resonance energy change can be also used to follow and interpret a ligand exchange procedure. We use the resonance peak broadening ($\Delta\Gamma$) of the prototypical, hexadecyltrimethylammonium bromide (CTAB)-covered gold nanorods upon thiol molecule binding to investigate how the ligand replacement at the gold nanoparticle interface evolves for two simple, similarly sized, but oppositely charged thiols − cysteamine and mercaptopropionic acid (MPA). We combine ensemble and single-particle methods to gain better insights into the different behavior of the two types of molecules.

EXPERIMENTAL SECTION

Hexadecyltrimethylammonium bromide (CTAB, 99%), hexadecyltrimethylammonium chloride (CTAC, 25 wt % in water), sodium borohydride ($NaBH_4$, 99%), hydrogen tetrachloroaurate trihydrate ($HAuCl_4$, 99,9%), sodium oleate (NaOl, ≥ 99%), silver nitrate ($AgNO_3$, >99%), hydrochloric acid (37%), L-ascorbic acid (AA, >99%), cysteamine hydrochloride (>99%), and MPA (≥99%) were obtained from Sigma-Aldrich. All chemicals were utilized as received. For all experiments, ultrapure water with a resistivity of 18.2 MΩcm was used.

The gold nanorods employed in this paper were prepared based on an earlier published seed-mediated protocol.[16] For ensemble optical and electrokinetic measurements, the as-prepared nanorods were washed twice with 50 mM CTAB, and after the third round 90% of the supernatant removed and redispersed with a certain concentration of thiol ligands, then gently stirred for 30 min. Afterward, the extinction spectra and the electrophoretic mobility of the solutions were obtained. To acquire the scattering spectra of single gold nanorods, we spin-coated particles on cleaned (15 min sonication in acetone, isopropanol, and water) glass slides. Excess surfactant was removed by immersing the substrates in isopropanol for 20 min. The cleaned substrates were integrated into a liquid cell (HybriWell HBW6021, GraceBiolabs), which was mounted in our laboratory-built optical workstation that allows the acquisition of individual particles' scattering spectra. It consists of an upright optical microscope (Olympus BX51), where the stage has been replaced with an XYZ piezo stage (Physik Instrumente, P-545.3R8S). The microscope is coupled to an aberration corrected imaging spectrograph (Princeton Instruments Isoplane SCT320 with PIXIS:400BRX −70 ° C cooled CCD camera). Dark-field illumination was performed using a 100 W light source (Olympus U-LH100IR) and an oil-immersion dark-field condenser (Olympus U-DCW, NA = 1.2−1.4). Our custom written Labview control software allows automatic positioning and autofocusing of the selected individual scatterer of interest using the spectrometer camera and the piezo stage. The outline of the measurement is shown in Scheme 1. First, ultrapure water was flushed extensively

Scheme 1. Schematics of the Experiment[a]

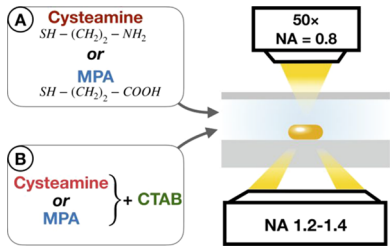

[a](A) The scattering spectrum of substrate-deposited individual gold nanorods is obtained and they were analyzed in a flow cell, 20 min after cysteamine or 3-mercapropionic acid (MPA) solutions were introduced. (B) In another set of experiments, the particles are first conditioned with CTAB after which thiols mixed with CTAB are introduced.

through the cell and the spectra of ca. 10 nanorods were measured with an exposure time of 2 s; these spectra were used as reference to assess the effect of the thiols. Then thiol solutions (MPA or cysteamine) with different concentrations in the range of 10^{-4} to 100 mM were flushed through the liquid cell subsequently and the same particles as before were measured again (Scheme 1A). We repeated the same procedure on a different set of particles in the presence of up to 5 mM CTAB solution as well; in this case, the reference spectra of the selected scatterers were obtained in the surfactant solution (Scheme 1B). Each measurement was carried out after 20 min contact time with the given thiol concentration. SEM images were obtained using a Zeiss LEO field-emission scanning electron microscope operated at 5 keV acceleration voltage.

RESULTS AND DISCUSSION

The synthesized nanorods have average dimensions of 76 × 24 nm with an aspect ratio of about 3.2. Their extinction spectrum is shown in Figure S1, and the longitudinal resonance peak is centered around 770 nm. Of note, for this aspect ratio and resonance wavelength, the width (damping) of the longitudinal plasmon resonance is not affected by the contribution related

https://dx.doi.org/10.1021/acs.jpcc.0c04629
J. Phys. Chem. C 2020, 124, 19736−19742

to interband transitions which take place at resonance energies higher than ∼1.76 eV (shorter wavelength than ∼705 nm).[6] Consequently, any change in linewidth can be attributed to the change in the surface damping/CID contribution. To investigate the impact of the short-chain thiols on the ligand exchange, ensemble measurement spectra have been taken as a function of the thiol concentration. In this case, however, the background concentration of CTAB is fixed at 5 mM to prevent aggregation of the rods. When cysteamine is added to the native sample, a similar trend is observed as reported earlier,[17] that is, the longitudinal peak position of the nanorods asymptotically blue-shifts, which is accompanied by the gradual increase of the electrophoretic mobility (Figure 1a). As the

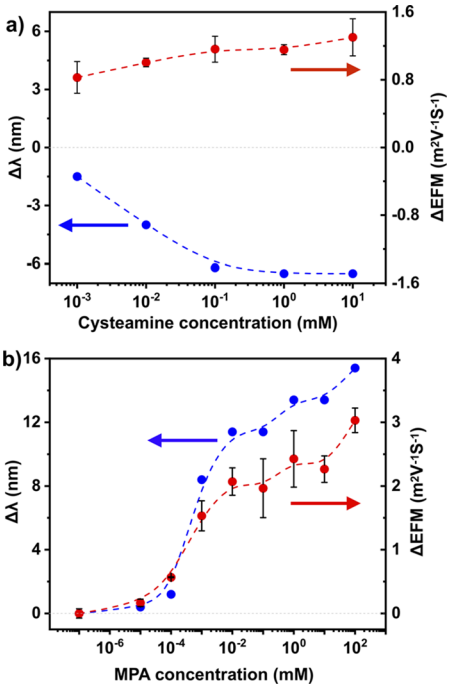

Figure 1. Longitudinal plasmon resonance peak shift ($\Delta\lambda$) and electrophoretic mobility change (ΔEFM) of the nanorods determined from ensemble measurements upon adding (a) cysteamine and (b) MPA to the as-prepared sample at 5 mM CTAB concentration.

shift of the longitudinal LSPR peak provides information primarily on changes in the dielectric properties of the tip region,[18] the observed blue shift can be attributed to the CTAB displacement at the nanorod tip region by the shorter chain cysteamine, leading to a lower average effective refractive index at the rods' ends. Above 10 mM cysteamine concentration, the sample loses its stability. Interestingly, when MPA is used for the ligand replacement, a gradual red shift is observed as a function of MPA concentration, which is accompanied by increasing mobility, which is a positive electrophoretic mobility change (Figure 1b). This finding is in stark contrast to the results obtained with cysteamine. At the pH of the solution (pH = 6.4) under experimental conditions, the cysteamine can be considered to be present in its protonated form (pK_a = 10.75), whereas the MPA is mainly deprotonated (pK_a = 4.3). Based on the ensemble measurements it can be argued that there is some interaction between the negatively charged MPA and the positively charged CTAB molecules, which then could lead to a significant increase of the effective refractive index in the tip region. Such a red shift has been previously experimentally observed for spherical, CTAB/C-capped nanospheres when interacted with MPA, but no explanation was given.[19] Earlier it was also argued, that MPA would electrostatically adhere to the surface-bound CTAB layer.[20] However, the extent of the red shift upon MPA addition observed in Figure 1b is unlikely to originate from the accumulation of a short-chain molecule adlayer in the outer region of the ligand shell, because of the exponentially decaying nature of the near-field. It is more probable that MPA molecules bind to the gold surface via their thiol groups, thus promoting the accumulation of additional CTAB molecules from the bulk. This would also explain the simultaneously observed electrophoretic mobility increase. To investigate this finding in detail, and to elucidate the origin of the different effect of the similarly sized, but oppositely charged cysteamine and MPA, the scattering spectra of individual nanorods have been measured and analyzed. This provides several additional benefits for addressing the problem. First, as the particles are deposited on a substrate, spectral changes can be investigated in a much broader concentration range without the danger of particle aggregation. Second, as the particles are immobilized on a substrate, the thiol binding experiments can be also decoupled for the CTAB bulk concentration and the spectroscopic measurements can be also carried out in pure water. Third, the binding of the thiol molecules can be independently confirmed by analyzing the scattering peak width of the individual particle's spectra.

As for the single-particle experiments, the particles are deposited on a substrate and mounted in a flow cell, and the bulk concentration of CTAB can be set to zero. The first set of experiments has been carried out on such a system, flushing the cells extensively with water to remove all CTAB from the bulk and allows the nanorods to equilibrate with the pure solvent. It is a question though to which extent CTAB can be removed, as there is experimental evidence that even if thiols are used for the ligand exchange, CTAB can remain on the surface of the rods. The measured scattering spectrum of a single nanorod is shown in Figure 2, fitted with a Lorentzian function in order to determine the resonance wavelength (Ω_{res}) and the homogeneous LSPR linewidth (Γ) of the resonance peak. Because we measured the same individual gold nanorods during the given surface modification process, we only need to consider changes in linewidth and resonance energy. For convenience, the obtained resonance energies were

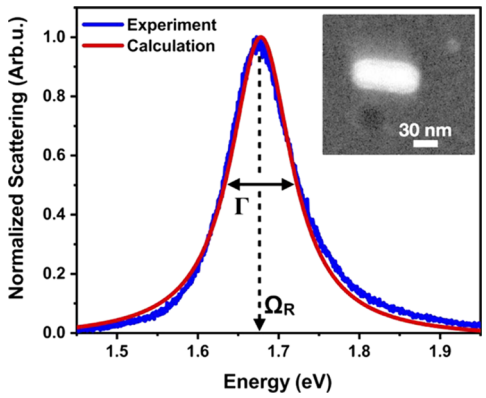

Figure 2. A representative scattering spectrum of an individual gold nanorod and its Lorentzian fit. The inset shows the SEM micrograph of the very same particle with dimensions of 31 × 79 nm.

https://dx.doi.org/10.1021/acs.jpcc.0c04629
J. Phys. Chem. C 2020, 124, 19736−19742

converted into resonance wavelengths and corresponding wavelength shifts. In the simplest case of an ideal rod, as the thiol molecules bind to the rod's surface, the increase of both the resonance wavelength and the peak width is expected because of the increasing effective refractive index and CID, respectively. Additionally, both the shift and broadening are anticipated to be proportional to the coverage of the rod by the thiols.

In Figure 3, the resonance wavelength and damping change values can be seen for the case where CTAB has been removed

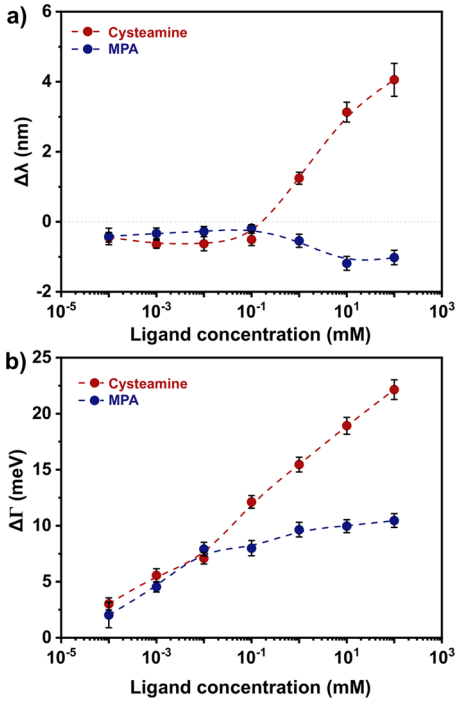

Figure 3. (a) Longitudinal resonance peak shift and (b) broadening obtained for cysteamine and MPA as a function of the thiol concentration.

from the bulk (examples of the actually measured spectra for cysteamine are provided in Figure S2). There is a striking difference between the effect of cysteamine and MPA. The two molecules have only a minor effect on the resonance wavelength from 10^{-4} up to 10^{-1} mM (although there might be a slight, opposite trend observable, with cysteamine inducing a small blue shift, while MPA shows a red shift, Figure 3a), above which a clearly opposite trend is observed. Cysteamine causes a significant red shift, while MPA causes a small blue shift. It has to be noted that this trend is the inverse to the changes observed during the ensemble bulk experiments shown in Figure 1, but in contrast to the bulk experiments in the flow cell, the concentration of CTAB has been set to zero. Although these finding are puzzling, the increase of the damping for both molecules (Figure 3b) clearly shows that both molecules indeed bind to the rods. There is also a characteristic difference in the concentration dependence for the two molecules. The binding of cysteamine proceeds over the whole investigated concentration range, whereas for MPA further accumulation seems to be inhibited starting from 0.1 mM (note the logarithmic abscissa). The findings can be explained based on two reasonable, interdependent assumptions. First, the surface of the rods has some physiosorbed CTAB present on their surface despite the extensive washing—an issue also reported in earlier studies.[7,11,21] Second, the charge of the molecule plays a crucial role in determining how the thiol binding takes place at the particle and how the short-chain thiol interacts with the CTAB molecule. It can be assumed that at low thiol concentrations the molecules will prefer easily accessible sites at the rod surface, that are either high energy binding sites or areas free of CTAB remnants. The electric interaction between the thiol functional group and CTAB results in two different scenarios. Binding of the positively charged cysteamine can lead to the CTAB leaving the interface, because the short molecule induces local charge repulsion but in contrast to CTAB cannot provide stabilization by intermolecular attraction caused by a large aliphatic tail. This leads to loosening of the remaining CTAB on the gold surface, and consequently there is a minimal blue shift up to 0.1 mM in Figure 3a for cysteamine, but as the particle is covered more extensively by the molecule, a clear red shift is obtained. According to Figure 3b, up to 0.1 mM, the binding of MPA commences in the same way, but then its further accumulation on the surface seems to be blocked compared to cysteamine. This might be again attributed to the interaction between MPA and the CTAB at the interface, which—opposite to cysteamine—is attractive and can provide additional stability to the original capping ligand. This leads to a self-limiting process, reducing the amount of MPA able to bind to the rod in the given time frame. Obviously, the large (ca. 185 kJ/mol)[22] binding energy of thiols wins over the physiosorbed and probably stabilized CTAB at higher MPA concentrations, leading to the removal of some CTAB from the surface and the observed small blue shift as shown in Figure 3a.

Even if the exact remaining coverage of the nanorods by the CTAB is not known, the above outlined hypothesis can be tested, when the CTAB concentration in the bulk is varied. As the CTAB concentration in the bulk approaches its critical micelle concentration (0.9 mM),[23] the structure of the native ligand layer will be that of a bilayer,[1] albeit some studies indicate the concentration dependent micellar structure of CTAB at the interface.[24,25] Figure 4 shows the result obtained at 5 mM CTAB concentration, that corresponds to the concentration level during the bulk experiments. The presence of CTAB in itself causes a significant, ca. 9 nm red shift of the longitudinal peak position (Figure S3a) compared to the cleaned nanorods, which is expected for the case of a developing CTAB layer at the particle interface. Hence, to obtain the respective peak position and damping values in the presence of CTAB, for each nanorod, the resonance spectra obtained after conditioning at the respective CTAB concentration were used as reference. Interestingly, a higher CTAB concentration leads to smaller initial damping values (Figure S3b). This is in qualitative agreement with recent results, where the CTAB concentration dependent damping change was attributed to the simultaneous variation in surface concentration of silver ions.[26] In our case, however, the effect of silver can be ruled out as only CTAB is added to the cleaned nanorods. It has to be emphasized, that irrespective of the CTAB concentration, the damping change is positive upon thiol binding in agreement with earlier literature results.[7−12]

It is clear that cysteamine now causes a large blue shift of the longitudinal mode (Figure 4a) − just as during the bulk experiments shown earlier (a side-by-side comparison of the CTAB impact in the case of cysteamine is provided in Figure

https://dx.doi.org/10.1021/acs.jpcc.0c04629
J. Phys. Chem. C 2020, 124, 19736−19742

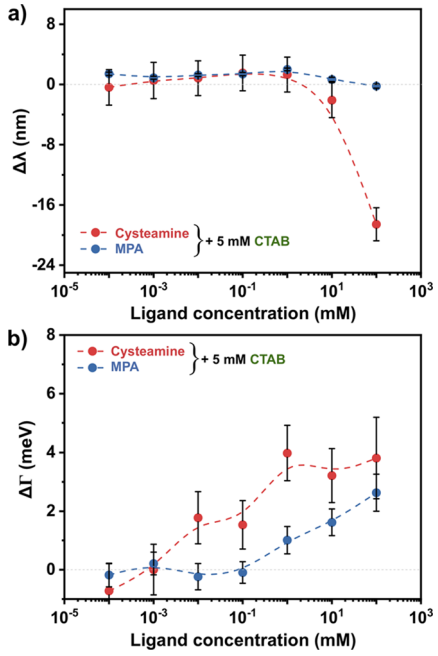

Figure 4. (a) Longitudinal resonance peak shift and (b) broadening obtained at 5 mM CTAB background concentration for cysteamine and MPA as a function of the thiol concentration.

S4). This is consistent with the CTAB replacement at the rod tips by cysteamine. Earlier findings have shown that cysteamine at 5 mM concentration is able to etch and shorten the nanorods at 60 °C in the presence of CTAB.[27] Although our experiments did not involve additional heating of the sample, contribution to the blue shift at large concentrations by the shortening of the rods cannot be ruled out a priori. As shown by some simulation results in Figure S5, shortening a 76 × 24 nm nanorod by 2 nm causes ca. 10 nm blue shift of the theoretical resonance wavelength. The pronounced accumulation of cysteamine on the rod is also shown by the increase of damping (Figure 4b).

It has to be pointed out that there is also a small red shift at lower concentrations that—based on the corresponding damping increase—are also a result of the cysteamine binding. This could correspond to the small molecule occupying accessible binding sites first without removing CTAB from the surface. For MPA, the LSPR peak position first slightly red-shifts, and then blue-shifts, but to a smaller extent than for cysteamine. This is also consistent with the smaller associated damping increase and underlines the possibility that the binding of MPA is limited by the stabilization of the CTAB layer by the readily bound thiol molecules. The above findings are summarized in Scheme 2. At low CTAB bulk concentration, cysteamine is able to effectively replace the initial ligands, while compared to this, the binding of MPA is limited (A). As the bulk CTAB concentration is increased, the binding of the thiols is gradually reduced (B). In the case of MPA, the binding of the thiol might result in the accumulation of additional CTAB at the rods' surface.

Scheme 2. Cartoons showing the possible differences and outcomes of the thiol binding when the ligand exchange is carried out (A) without adding CTAB and (B) at increasing CTAB concentration

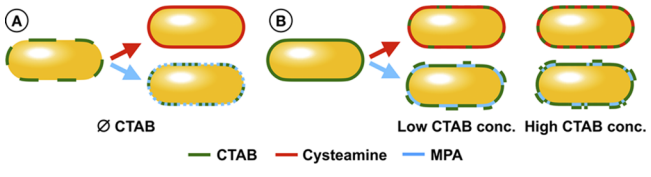

To gain deeper insights into this effect, experiments were carried out for the case when MPA was used as surface modification ligand at an intermediate CTAB concentration level. In this case, the bilayer structure of the CTAB layer cannot be anticipated anymore. The associated resonance wavelength change at intermediate (10^{-3} mM) CTAB concentration follows a similar trend as earlier (see Figure 5a). On the other hand, the magnitude of the wavelength shift

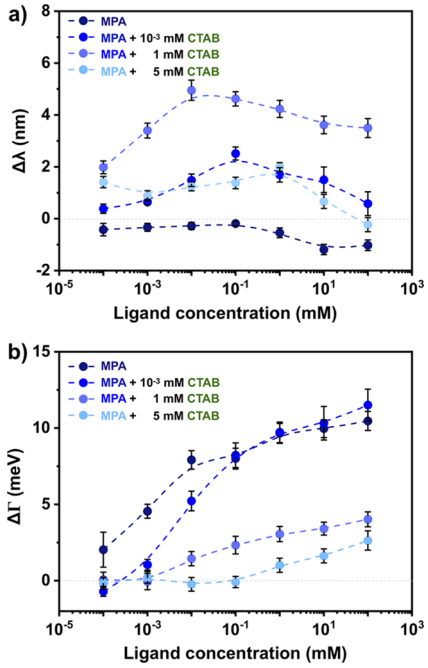

Figure 5. (a) MPA-induced longitudinal resonance peak shifts and (b) broadening obtained at different CTAB background concentration levels

in general is clearly proportional to the bulk CTAB concentration up to 1 mM CTAB concentration. This indicates already that CTAB binding to the partially surface-modified nanorod plays an important role in the process. Comparing the damping changes (Figure 5b) obtained at different CTAB background concentration levels reveals that at 10^{-3} mM surfactant concentration, MPA binding is suppressed in the lower concentration range (below 10^{-1} mM), but is virtually the same at higher concentration as the one obtained without CTAB in the bulk. This indicates that there might be a higher amount of CTAB present at the rod's surface that can inhibit MPA accumulation to some extent when MPA is applied at a very low concentration. When the MPA binding process occurs in the presence of 1 mM CTAB solution, the increase of the damping remains also suppressed but in the entire investigated concentration range. All the curves above the 10^{-1} mM MPA concentration become parallel which implies the similar inhibition mechanism of the CTAB molecules when the binding of the ligand on the surface of the nanorod is blocked. This also holds for the 5 mM CTAB case, for which the binding of MPA is even more suppressed:

https://dx.doi.org/10.1021/acs.jpcc.0c04629
J. Phys. Chem. C 2020, 124, 19736−19742

the damping change is generally smaller and its increase becomes significant only above ca. 0.1 mM MPA concentration. The suppressed accumulation of MPA is reflected in the lower red shifts compared to the 1 mM CTAB case (Figure 5a).

Conclusions. The localized resonance peak broadening (resonance damping increase) of individual gold nanorods upon thiol binding was found to be a useful indicator to describe the ligand exchange process at the particles' surface, especially when combined with the information on the corresponding peak position shifts and ensemble measurement results. The two molecules—cysteamine and MPA—investigated in the present study both clearly bind to the gold particles as shown by the increasing damping. There is a clear difference between the two ligands that can be interpreted by the different interaction of the thiol and the native CTAB layer of the rods. MPA stabilizes the particles' native CTAB layer because of their interaction, resulting in a lower binding especially at higher concentration. This is corroborated by the finding that the stabilizing effect also scales with the CTAB concentration, and, for the negatively charged MPA, a pronounced red shift is observed. The latter indicates that in spite of the molecule binding to gold, it does not remove the CTAB completely from the particles' vicinity, which suggests that the CTAB is still physically bound to the MPA-modified surface. Based on the damping increase, adsorption of the positively charged cysteamine is more pronounced. The absence of the pronounced red shift indicates a more complete CTAB removal, and hence it can be considered as more effective in destabilizing the CTAB layer. The results obtained for these simple systems highlight the central role of intermolecular forces in the surface modification process. They can be a key factor even in the case when there is a large difference in the intrinsic binding energy of the competing molecule types, and could result in a significant amount of original capping ligand present is the system even after "complete" ligand exchange. It is also clear that, in general, when the LSPR surface damping effect is studied for different types of ligands and semiempirical surface damping (A) and CID (A_{CID}) parameters are compared for different systems, the capping layer composition around the nanoparticles has to be carefully considered.

■ ASSOCIATED CONTENT

Supporting Information

The Supporting Information is available free of charge at https://pubs.acs.org/doi/10.1021/acs.jpcc.0c04629.

Ensemble extinction spectrum of the synthesized nanorods, characteristic single nanorod scattering spectra, the intrinsic effect of CTAB on the damping and resonance wavelength and upon cysteamine addition at different CTAB background concentrations, and optical simulation details and results (PDF)

■ AUTHOR INFORMATION

Corresponding Author

András Deák − *Institute of Technical Physics and Materials Science, Centre for Energy Research, H-1525 Budapest, Hungary*; orcid.org/0000-0002-2526-1245; Email: andras.deak@energia.mta.hu

Authors

Dániel P. Szekrényes − *Institute of Technical Physics and Materials Science, Centre for Energy Research, H-1525 Budapest, Hungary*

Dávid Kovács − *Institute of Technical Physics and Materials Science, Centre for Energy Research, H-1525 Budapest, Hungary*

Zsolt Zolnai − *Institute of Technical Physics and Materials Science, Centre for Energy Research, H-1525 Budapest, Hungary*

Complete contact information is available at: https://pubs.acs.org/10.1021/acs.jpcc.0c04629

Author Contributions

The manuscript was written through contributions of all authors. All authors have given approval to the final version of the manuscript.

Notes

The authors declare no competing financial interest.

■ ACKNOWLEDGMENTS

The project was supported by the Hungarian Scientific Research Fund FK-128327 and KH-129578. D.P. Sz. acknowledges the support of the Pro Progressio and József Varga Foundations.

■ REFERENCES

(1) Burrows, N. D.; Lin, W.; Hinman, J. G.; Dennison, J. M.; Vartanian, A. M.; Abadeer, N. S.; Grzincic, E. M.; Jacob, L. M.; Li, J.; Murphy, C. J. Surface Chemistry of Gold Nanorods. *Langmuir* **2016**, *32*, 9905−9921.

(2) Zhang, Q.; Hernandez, T.; Smith, K. W.; Hosseini Jebeli, S. A.; Dai, A. X.; Warning, L.; Baiyasi, R.; McCarthy, L. A.; Guo, H.; Chen, D.-H.; et al. Unraveling the Origin of Chirality from Plasmonic Nanoparticle-Protein Complexes. *Science* **2019**, *365*, 1475−1478.

(3) Zhu, H.; Xie, H.; Yang, Y.; Wang, K.; Zhao, F.; Ye, W.; Ni, W. Mapping Hot Electron Response of Individual Gold Nanocrystals on a TiO_2 Photoanode. *Nano Lett.* **2020**, *20*, 2423−2431.

(4) Hu, M.; Novo, C.; Funston, A.; Wang, H.; Staleva, H.; Zou, S.; Mulvaney, P.; Xia, Y.; Hartland, G. V. Dark-Field Microscopy Studies of Single Metal Nanoparticles: Understanding the Factors That Influence the Linewidth of the Localized Surface Plasmon Resonance. *J. Mater. Chem.* **2008**, *18*, 1949.

(5) Sönnichsen, C.; Franzl, T.; Wilk, T.; von Plessen, G.; Feldmann, J. Drastic Reduction of Plasmon Damping in Gold Nanorods. *Phys. Rev. Lett.* **2002**, *88*, 077402.

(6) Foerster, B.; Rutten, J.; Pham, H.; Link, S.; Sönnichsen, C. Particle Plasmons as Dipole Antennas: State Representation of Relative Observables. *J. Phys. Chem. C* **2018**, *122*, 19116−19123.

(7) Foerster, B.; Spata, V. A.; Carter, E. A.; Sönnichsen, C.; Link, S. Plasmon Damping Depends on the Chemical Nature of the Nanoparticle Interface. *Sci. Adv.* **2019**, *5*, eaav0704.

(8) Lee, S. Y.; Tsalu, P. V.; Kim, G. W.; Seo, M. J.; Hong, J. W.; Ha, J. W. Tuning Chemical Interface Damping: Interfacial Electronic Effects of Adsorbate Molecules and Sharp Tips of Single Gold Bipyramids. *Nano Lett.* **2019**, 2568.

(9) Seo, M. J.; Kim, G. W.; Tsalu, P. V.; Moon, S. W.; Ha, J. W. Role of Chemical Interface Damping for Tuning Chemical Enhancement in Resonance Surface-Enhanced Raman Scattering of Plasmonic Gold Nanorods. *Nanoscale Horiz* **2020**, 345.

(10) Liyanage, T.; Nagaraju, M.; Johnson, M.; Muhoberac, B. B.; Sardar, R. Reversible Tuning of the Plasmoelectric Effect in Noble Metal Nanostructures Through Manipulation of Organic Ligand Energy Levels. *Nano Lett.* **2020**, *20*, 192−200.

(11) Foerster, B.; Joplin, A.; Kaefer, K.; Celiksoy, S.; Link, S.; Sönnichsen, C. Chemical Interface Damping Depends on Electrons Reaching the Surface. *ACS Nano* **2017**, *11*, 2886−2893.
(12) Moon, S. W.; Tsalu, P. V.; Ha, J. W. Single Particle Study: Size and Chemical Effects on Plasmon Damping at the Interface between Adsorbate and Anisotropic Gold Nanorods. *Phys. Chem. Chem. Phys.* **2018**, *20*, 22197−22202.
(13) Therrien, A. J.; Kale, M. J.; Yuan, L.; Zhang, C.; Halas, N. J.; Christopher, P. Impact of Chemical Interface Damping on Surface Plasmon Dephasing. *Faraday Discuss.* **2019**, *214*, 59−72.
(14) Jeon, H. B.; Ha, J. W. Single-Particle Study: Plasmon Damping of Gold Nanocubes with Vertices by Adsorbate Molecules: Single-Particle Study: Plasmon Damping of Gold Nanocubes with Vertices by Adsorbate Molecules. *Bull. Korean Chem. Soc.* **2018**, *39*, 1117−1119.
(15) Zijlstra, P.; Paulo, P. M. R.; Yu, K.; Xu, Q.-H.; Orrit, M. Chemical Interface Damping in Single Gold Nanorods and Its Near Elimination by Tip-Specific Functionalization. *Angew. Chem., Int. Ed.* **2012**, *51*, 8352−8355.
(16) Ye, X.; Zheng, C.; Chen, J.; Gao, Y.; Murray, C. B. Using Binary Surfactant Mixtures To Simultaneously Improve the Dimensional Tunability and Monodispersity in the Seeded Growth of Gold Nanorods. *Nano Lett.* **2013**, *13*, 765−771.
(17) Szekrenyes, D. P.; Pothorszky, S.; Zambo, D.; Osváth, Z.; Deák, A. Investigation of Patchiness on Tip-Selectively Surface Modified Gold Nanorods. *J. Phys. Chem. C* **2018**, *122*, 1706−1710.
(18) Antosiewicz, T. J.; Köll, M. A Multiscale Approach to Modeling Plasmonic Nanorod Biosensors. *J. Phys. Chem. C* **2016**, *120*, 20692−20701.
(19) Dewi, M. R.; Laufersky, G.; Nann, T. A Highly Efficient Ligand Exchange Reaction on Gold Nanoparticles: Preserving Their Size Shape and Colloidal Stability. *RSC Adv.* **2014**, *4*, 34217−34220.
(20) Garabagiu, S.; Bratu, I. Thiol Containing Carboxylic Acids Remove the CTAB Surfactant onto the Surface of Gold Nanorods: An FTIR Spectroscopic Study. *Appl. Surf. Sci.* **2013**, *284*, 780−783.
(21) Indrasekara, A. S. D. S.; Wadams, R. C.; Fabris, L. Ligand Exchange on Gold Nanorods: Going Back to the Future. *Part. Part. Syst. Charact.* **2014**, *31*, 819−838.
(22) Pensa, E.; Cortés, E.; Corthey, G.; Carro, P.; Vericat, C.; Fonticelli, M. H.; Benítez, G.; Rubert, A. A.; Salvarezza, R. C. The Chemistry of the Sulfur−Gold Interface: In Search of a Unified Model. *Acc. Chem. Res.* **2012**, *45*, 1183−1192.
(23) Li, W.; Zhang, M.; Zhang, J.; Han, Y. Self-Assembly of Cetyl Trimethylammonium Bromide in Ethanol-Water Mixtures. *Front. Chem. China* **2006**, *1*, 438−442.
(24) Meena, S. K.; Celiksoy, S.; Schäfer, P.; Henkel, A.; Sönnichsen, C.; Sulpizi, M. The Role of Halide Ions in the Anisotropic Growth of Gold Nanoparticles: A Microscopic Atomistic Perspective. *Phys. Chem. Chem. Phys.* **2016**, *18*, 13246−13254.
(25) González-Rubio, G.; Díaz-Núñez, P.; Rivera, A.; Prada, A.; Tardajos, G.; González-Izquierdo, J.; Bañares, L.; Llombart, P.; Macdowell, L. G.; Alcolea Palafox, M.; Liz-Marzán, L. M.; Peña-Rodríguez, O.; Guerrero-Martínez, A. Femtosecond Laser Reshaping Yields Gold Nanorods with Ultranarrow Surface Plasmon Resonances. *Science* **2017**, *358*, 640−644.
(26) Ye, W.; Krüger, K.; Sánchez-Iglesias, A.; García, I.; Jia, X.; Sutter, J.; Celiksoy, S.; Foerster, B.; Liz-Marzán, L. M.; Ahijado-Guzmán, R.; Sönnichsen, C. CTAB Stabilizes Silver on Gold Nanorods. *Chem. Mater.* **2020**, *32*, 1650−1656.
(27) Szychowski, B.; Leng, H.; Pelton, M.; Daniel, M.-C. Controlled Etching and Tapering of Au Nanorods Using Cysteamine. *Nanoscale* **2018**, *10*, 16830−16838.

https://dx.doi.org/10.1021/acs.jpcc.0c04629
J. Phys. Chem. C 2020, 124, 19736−19742